The clear sky brightness near the horizon: few-parameter models and comparison with experiment

I.M. Nasrtdinov, T.B. Zhuravleva, and S.M. Sakerin

Institute of Atmospheric Optics,
Siberian Branch of the Russian Academy of Sciences, Tomsk

Received April 27, 2006

Few-parameter descriptions of distribution of the near-horizon brightness fields are presented, which are based on model calculations for aerosol–gaseous spherical atmosphere. The results of numerical simulation are compared with experimental data. A new method of determination of the aerosol optical depth (AOD) from measurements of near-horizon sky brightness is suggested. The advantage of this method is that it does not require the absolute calibration of instruments: AOD is retrieved from relative measurements of the angular position of the sky brightness maximum.

Introduction

The brightness distribution over sky is often required when solving a number of direct and inverse problems of atmospheric optics. A large cycle of theoretical and experimental studies of the daylight sky brightness was performed at the Astrophysical Institute, Almaty (see, e.g., Ref. 1). The studies revealed main regularities and factors determining the brightness distribution over sky. It is found that the sky brightness in its different areas can differ from 5 to 2000 times, depending on the spectral range and position of Sun. However, these works insufficiently fully describe the sky brightness for viewing zenith angles larger than ~ 80°.

Description of the sky brightness field on the basis of experimental studies is difficult, because it requires long-term observations under conditions of a large variety of atmospheric situations. Therefore, methods of numerical simulation[2–7] are widely used in recent years for this purpose, allowing one to solve the radiation transfer equation for scattering and absorbing media with a satisfactory accuracy. Most developed algorithms were constructed under the assumption of the plane-parallel model of the atmosphere, and found their application in methods of determination of aerosol optical characteristics, e.g., retrieval of the single scattering albedo (SSA) for the entire atmospheric column.[8–10] One of the limitations of these methods is that they are inapplicable to the Sun and/or viewing zenith angles larger than about 80° (Refs. 6 and 7). For large zenith angles, the calculation algorithms for spherical model of the atmosphere were developed,[5–7] one of which was modified[11,12] and used in our investigations. Using this algorithm, a numerical model of the sky brightness field was constructed and main regularities in formation of its angular structure in the near-horizon sky area were revealed.[13]

To solve the radiation transfer equation by the methods of numerical simulation, it is necessary to know a large number of input parameters, which may not always be accessible (such as altitude profiles of aerosol characteristics). In this regard, for problems, not requiring a high accuracy, it is useful to construct few-parameter models (FPMs) for scattered radiation fields. The most known model is the analytical description of brightness distribution over sky by Sobolev.[14] The model has a satisfactory accuracy for a wide range of input parameters; however, it becomes practically unacceptable at zenith angles larger than 80°. Other FPMs can be found in Ref. 15. They treat the zenith–azimuthal behavior of the sky brightness in more detail; however, they are also inapplicable to the region of the horizon.

In this paper we present few-parameter models of the angular dependence of the near-horizon sky brightness, as well as estimates of their accuracy. Based on one of the models, we suggest a new method of determination of atmospheric aerosol optical depth τ_{aer} (AOD) from the angular position of the sky brightness maximum above the horizon. To test the performed radiation calculations and the method, we compare numerical calculations with results of field measurements.

1. Comparison of results of numerical and field experiments

The comparison of our results with those of other authors is presented in Ref. 11, where their good agreement has been shown. To test the adequacy of the algorithm and revealed regularities,[13] we now compare the model calculations with data of field experiment. Remind that the chosen numerical approach is based on the use of the Monte Carlo method and a series of exponentials.[12] The algorithm makes it possible to take into account the vertical inhomogeneity and sphericity of the atmosphere,[11] aerosol–molecular scattering and absorption, reflection from underlying surface, and the actual instrumental function of photometers.

0235-6880/06/10 804-07 $02.00

1.1. Characterization of instrumentation and experimental conditions

In summer periods of 2003–2005, we studied experimentally angular distributions of diffuse radiation in the clear sky. Measurements were performed in the forested zone ("Background" testing area of IAO SB RAS) 60 km away from Tomsk and included three types of experiments: 1) the study of azimuthal distribution of sky brightness in solar almucantar; 2) the same near the horizon; 3) the study of sky brightness as a function of the viewing zenith angle.

The sky brightness was measured by a scanning photometer, developed on the basis of the standard camera objective MTO-1000 and a two-coordinate rotable device. Individual spectral intervals were separated using interference filters installed in a continuously rotating drum. Some scanning photometer specifications are presented below. The experiments included measurements of atmospheric AOD in the range 0.37–1.06 μm with the sun photometer. The method of AOD calculation from sun photometer signals is described in Refs. 1 and 16.

Field of view Ω, deg.	0.25
Maxima of	0.44; 0.5; 0.63;
filter passband λ, μm	0.87; 1.06
Angular range of scans, deg.:	
in azimuth φ	0–360
in zenith ξ	50–97
Duration of one measurement cycle, min:	
in azimuth	3
in zenith	0.7

The instrumentation was located on the specially equipped tower at a height of 18 m above the ground. The forest tree height in the region of measurements was 17–25-m; therefore, for certain azimuths the measurements were possible only up to zenith angles of 88°.

To determine absolute values of the sky brightness, the photometer calibration was conducted through additional measurements of brightness of the diffuse (orthotropic) screen B_{scr}, oriented perpendicularly to the incident direct radiation.[1,17] In this case, for recorded radiation fluxes $\Phi(\mu)$ from the sky and the screen Φ_{scr} we can write:

$$\Phi(\mu) = B(\mu)\Omega A_{in}, \quad (1)$$

$$\Phi_{scr} = B_{scr}\Omega A_{in} = \frac{R}{\pi} I_{\perp}\Omega A_{in}, \quad (2)$$

where $I_{\perp} = I_0 T^{atm}$ is the illumination of the perpendicular area by the direct radiation; Ω is the photometer field of view; I_0 is the extraterrestrial solar constant; R is the reflection coefficient of the screen; T^{atm} is the atmosphere transmission; A_{in} is the area of the photometer receiving system; μ is the cosine of the scattering angle θ uniquely connected with geometrical parameters of the experiment:

$$\mu = \sin\xi \sin\xi_0 \cos\varphi + \cos\xi \cos\xi_0, \quad (3)$$

ξ_0 is the solar zenith angle; and φ is the azimuth angle with respect to the Sun. From Eq. (1) and (2) we obtain the formula for the sky brightness:

$$B(\mu) = \frac{\Phi(\mu)R}{\Phi_{scr}\pi} I_{\perp}. \quad (4)$$

Further, the experimental dependences $B(\mu)$ were compared with results of numerical calculations taking into account the measured AOD values and other characteristics specified in the model. The aerosol scattering phase function $g_{aer}(\theta)$, aerosol single scattering albedo Λ_{aer}, and their spectral behaviors, used in the calculations, were specified in accordance with the standard WCP model[18] for the continental aerosol and midlatitude summer. The surface albedo A_S was assumed equal to 0.15. The molecular absorption coefficients were calculated using the spectroscopic database HITRAN-2000 on the basis of AFGL model[19] for the midlatitude summer.

1.2. Results of comparison of experimental and calculated angular distributions of the sky brightness

First we consider the dependence of diffuse radiation on the viewing zenith angle. Earlier it was shown[13] that the sky brightness may have nonmonotone dependence on the zenith angle with maximum in angular region $\xi = 80–90°$. Figure 1 illustrates the character of transformation of angular distributions of the sky brightness at varied τ_{aer}; and Figure 2 gives examples of comparison of model calculations with experimental dependences.

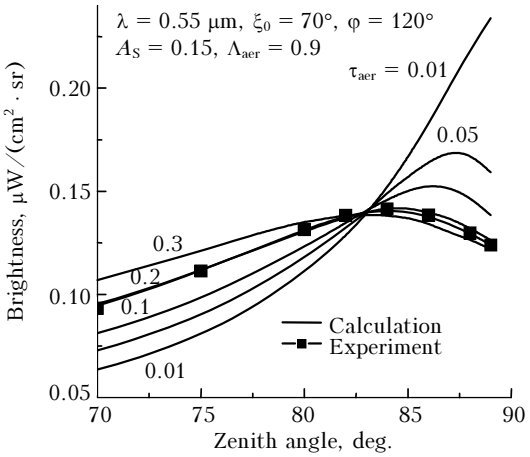

Fig. 1. Transformation of angular distribution of the sky brightness at variations of atmospheric AOD.

Model calculations and experimental tests have shown that the position of the brightness maximum depends on the total atmospheric optical depth τ:

$$\tau = \tau_{aer} + \tau_R,$$

where τ_R is the molecular scattering optical depth. As an example, Figure 2*b* presents a comparison of $B(\xi)$, calculated for different wavelengths: $\tau_{aer} = 0.1$, $\tau_R = 0.146$, $\tau = 0.246$ ($\lambda = 0.5$ μm) (*1*); and $\tau_{aer} = 0.23$,

$\tau_R = 0.015$, $\tau = 0.245$ ($\lambda = 0.87$ μm) (*2*). Figure 2*b* shows that for equal τ the angular position of the brightness maximum is the same. For this and other cases the comparison has shown a qualitatively satisfactory agreement between results of numerical and field experiments. Discrepancies generally do not exceed 20% and are caused by an inaccuracy of setting of model values of the aerosol SSA, the surface albedo, and the aerosol scattering phase function.

Comparison of azimuthal distributions of sky brightness $B(\varphi)$ on the horizon has shown that in most cases the results well agree (Fig. 3). However, in some cases the difference from numerical results can reach 25% (Fig. 3*b*). These differences are associated primarily with inaccuracy in the setting of model scattering phase function for aerosol, whose elongation primarily affects the azimuthal dependence $B(\varphi)$.

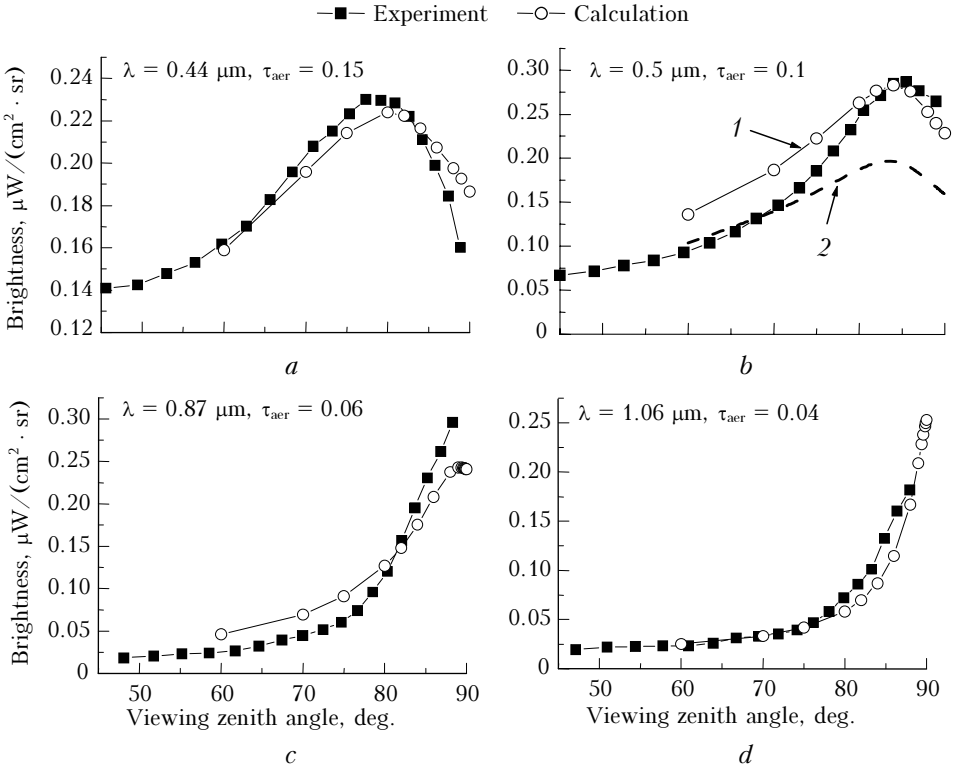

Fig. 2. Sky brightness versus viewing zenith angle: comparison of experimental data with results of numerical simulation ($\varphi = 150°$).

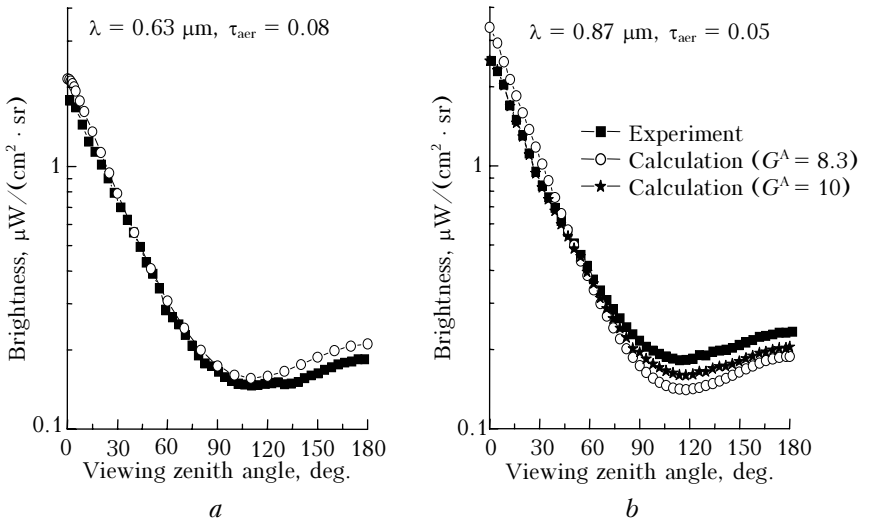

Fig. 3. Azimuthal sky brightness: comparison of experimental data and numerical simulation results.

In calculations exemplified by Fig. 3*b* we used the scattering phase function with the asymmetry factor $G^{\mathrm{A}} = 8.3$ ($G^A = \int_0^{\pi/2} g_{\mathrm{aer}}(\mu)\,\mathrm{d}\mu \Big/ \int_{\pi/2}^{\pi} g_{\mathrm{aer}}(\mu)\,\mathrm{d}\mu$). When another scattering phase function ($G^{\mathrm{A}} = 10$) is used, the differences decrease to 10%. It may appear that the brightness asymmetry decreases with growing G^{A}. The point is that the used scattering phase functions have different angular structures. The scattering phase function with an asymmetry factor of 8.3 has an overestimated backward hemisphere, while at $G^{\mathrm{A}} = 10$ the aureole part is too high; they are not shown in the figure because cannot be realized at the given geometry.

On the whole, the results of experimental testing have shown that the constructed algorithm correctly reflects the actual regularities of the diffuse radiation angular distribution at large viewing zenith angles and can be used for simulation of radiation transfer in the atmosphere.

2. Few-parameter representations of sky brightness angular distributions

Based on the revealed regularities and factors, affecting brightness distributions on the horizon,[13] we have constructed few-parameter models describing the azimuthal dependence of sky brightness beyond the solar aureole, as well as the position and magnitude of the brightness maximum above the skyline. Coefficients in the approximation formulas of azimuthal dependences of sky brightness and its multiple-scattering component were obtained for a spectral interval of 0.55 μm.

2.1. Model of sky brightness on the horizon (azimuthal dependence)

The calculations have shown that the corridor of possible brightness values $B_{\mathrm{H}}(\varphi)$ is a few tens of a percent if the optical characteristics vary practically throughout entire range of their actual variability: τ_{aer} between 0.05 and 0.4; Λ_{aer} between 0.8 and 1; the scattering phase function elongation $g_{\mathrm{aer}}(\theta)$ between 5 and 10; and the surface albedo between 0 and 0.7. Most influence on the sky brightness azimuthal dependence, especially in the forward hemisphere, is exerted by the aerosol scattering phase function, whose elongation is determined by the asymmetry factor G^{A} or the mean cosine $\bar{\mu}$. Therefore, to describe the angular structure of $B_{\mathrm{H}}(\theta)$, it is suggested to use the Henyey–Greenstein scattering phase function $g_{\mathrm{HG}}(\theta)$ with the mean cosine corresponding to $g_{\mathrm{aer}}(\theta)$. Other parameters affecting $B_{\mathrm{H}}(\theta)$ are the atmospheric aerosol optical depth and the optical mass m in the direction to Sun. Relatively weak sensitivity of $B_{\mathrm{H}}(\theta)$ to variations of other characteristics has made it possible to use their mean model values in the FPM construction. For convenience of presentation, the sky brightness angular dependence is given by the function of μ:

$$B_{\mathrm{H}}(\mu) = I_0 g_{\mathrm{HG}}(\mu)(a + b\mu)(c + d\mu^2); \qquad (5)$$

$$a = 0.09 + 1.51e^{-m/3} +$$

$$+1.25\exp\left[-12(1 - 0.1m + 0.009m^2)\tau\right];$$

$$b = 0.077 + 0.91e^{-m/3.85} + \left(1.36 + 6.42e^{-m/2.6}\right)\times$$

$$\times\exp\left[-(23.3 - 2.7m + 0.17m^2)\tau\right];$$

$$c = 0.55 + \tau; \quad d = 0.85 - 2\tau;$$

$$g_{\mathrm{HG}}(\mu) = 0.5\left(1 - \bar{\mu}^2\right)\left(1 - 2\mu\bar{\mu} + \bar{\mu}^2\right)^{-1.5},$$

$$\bar{\mu} = \int_{-1}^{1} g_{\mathrm{aer}}(\mu)\,\mu\mathrm{d}\mu.$$

Numerical parameters are calculated for mean (model) values $\Lambda_{\mathrm{aer}} = 0.9$ and $A_{\mathrm{S}} = 0.15$. The transformation of $B_{\mathrm{H}}(\mu)$ into dependence on the azimuth angle φ is made using formula (3):

$$\varphi = \arccos[(\mu - \cos\xi\cos\xi_0)/\sin\xi\sin\xi_0].$$

The Aerosol Robotic Network (AERONET) data suggest[20] that, for the last four years (2002–2005) in Tomsk, in 90% of cases the single scattering albedo varied from 0.85 to 0.99, and mean cosine varied from 0.6 to 0.68. The variability range of atmospheric AOD was 0.05–0.25 (Ref. 21). For the Henyey–Greenstein scattering phase function the change of the mean cosine from 0.6 to 0.68 corresponds to variability range 6.5–10 of the asymmetry factor G^{A}.

To estimate the error of model (5), we calculated the brightness by the Monte Carlo method and compared the result with calculations by formula (5). At exactly set input parameters ($\bar{\mu} = 0.64$; $\Lambda_{\mathrm{aer}} = 0.9$; $A_{\mathrm{S}} = 0.15$; $\tau_{\mathrm{aer}} = 0.15$; $\xi_0 = 75°$), the error for (5) is less than 10%. Since different $\bar{\mu}$, Λ_{aer}, and A_{S} can be realized in nature and model (5) is obtained for their means, then it is necessary to estimate the sensitivity of Eq. (5) to inaccuracy in assignment these parameters. To do this, we calculated the brightness distributions $B_{\mathrm{H}}(\mu)$ for different aerosol scattering phase functions $g_{\mathrm{aer}}(\mu)$ ($G^{\mathrm{A}} = 6.5$–10 or $\bar{\mu} = 0.6$–0.68), aerosol SSA (0.85–1.0), and A_{S} (0.1–0.2). The comparison of results has shown (Fig. 4*a*) that the error in the developed model does not exceed 20% (see error bars). In some cases, it may reach 35%. Figure 4*a* presents an example of such a realization for $A_{\mathrm{S}} = 0.2$, $\Lambda_{\mathrm{aer}} = 1.0$, $\tau_{\mathrm{aer}} = 0.15$, $\bar{\mu} = 0.68$, $\xi_0 = 75°$ (circles).

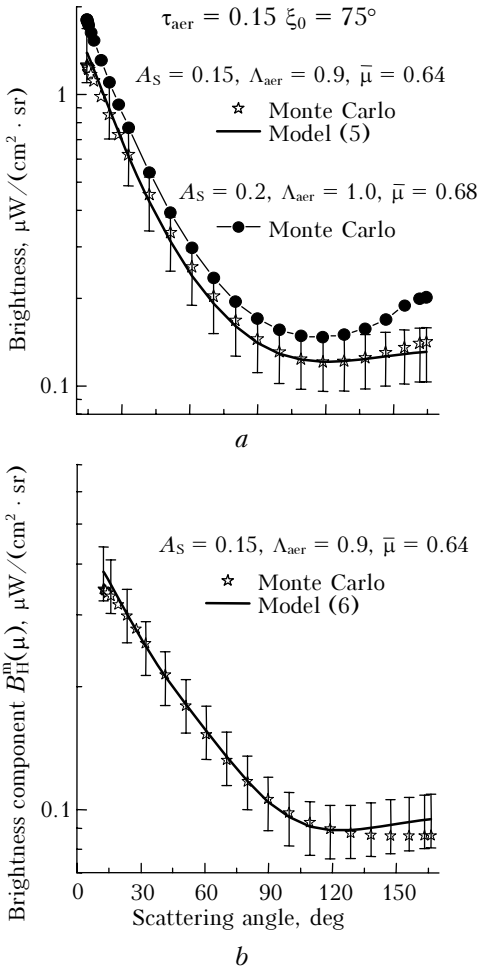

Fig. 4. Comparison of calculations of the sky brightness azimuthal dependence $B_H(\mu)$ with model (5) (*a*) and of the multiple-scattering component $B_H^m(\mu)$ with model (6) (*b*).

2.2. Parameterization of the sky brightness component due to multiple scattering $B_H^m(\mu)$ for the case of conservative scattering

The angular $B_H^m(\mu)$ pattern can be approximated with the help of the atmospheric scattering phase function in the form of the weighted sum of the molecular scattering phase function and the Henyey–Greenstein scattering phase function. More detailed consideration of the angular dependence can be made through introduction of an additional factor representing the third-order polynomial of μ:

$$B_H^m(\mu) = I_0 g(\mu)\left(a + b\mu + c\mu^2 + d\mu^3\right), \qquad (6)$$

where parameters *a*, *b*, *c*, and *d* are expressed in terms of elementary functions of τ_{aer} and *m*:

$$a = 0.038 + 0.06\tau_{aer} + (0.174 + 2.057\tau_{aer}) \times$$
$$\times \exp[-(0.115 + 0.458\tau_{aer})m],$$
$$b = 0.072 - 0.437\tau_{aer} - (0.005 - 0.02\tau_{aer})m;$$
$$c = -\left[0.025 + 0.012\tau_{aer} + (0.094 + 1.058\tau_{aer}) \times \right.$$
$$\left. \times \exp\left(-(0.122 + 0.448\tau_{aer})m\right)\right];$$
$$d = -\exp\left[-\left(1.29 + 3.097\tau_{aer} - (0.014 + 0.491\tau_{aer})m\right)\ln 10\right];$$
$$g(\mu) = \frac{g_{HG}(\mu)\tau_{aer} + g_R(\mu)\tau_R}{\tau_{aer} + \tau_R}, \quad g_R(\mu) = 0.375(1 + \mu^2).$$

Expansion constants (in parameters *a*, *b*, *c*, and *d*) were calculated for mean values of $g_{aer}(\theta)$ and A_S elongation. As in section 2.1, we compared model (6) with numerical calculations. The error of approximation formula (6) for exactly set input parameters also does not exceed 10% (Fig. 4*b*). Variations of atmospheric parameters in the same spectral range (see section 2.1) result in 15% error in calculation of $B_H^m(\mu)$.

2.3. Parameterization of the sky brightness maximum observed near the horizon

Analysis of sky brightness zenith distributions beyond the solar aureole ($\theta > 20°$) revealed the presence of the brightness maximum in the near-horizon zone ($\xi = 80$–$90°$), whose characteristics (position of ξ_{max} and magnitude of B_{max}) depend primarily on the total optical depth τ. For the given geometry of the experiment (*m*, φ) and the wavelength (or the molecular scattering depth), ξ_{max} is well approximated by the linear dependence on τ:

for the forward hemisphere

$$\xi_{max} = \min\{89.5 + 7e^{-\varphi/60} - (29.7 + 0.8m - 0.11\varphi)\tau; 90°\}, \qquad (7a)$$

for the backward hemisphere

$$\xi_{max} = \min\{89.5 + 7e^{-\varphi/60} - (14.2 + 0.9m + 0.04\varphi)\tau; 90°\}, \qquad (7b)$$

where the azimuth φ is given in degrees. It is seen that the position of ξ_{max} changes as a function of azimuth. Limiting angular position of the brightness maximum, which is realized under conditions of high atmospheric transmission ($\tau < 0.05$) is in the direction towards the horizon $\xi_{max} = 90°$. The calculations have shown that at variation of other optical characteristics (A_S from 0 to 0.3, $\Lambda_{aer} > 0.8$, G^A from 5 to 10), the error in ξ_{max} determination by the derived formulas does not exceed 1%.

For parameterization of the brightness B_{max} itself, it is possible to use the Henyey-Greenstein scattering phase function $g_{HG}(\mu)$ and an additional input parameter, i.e., approximate value of aerosol SSA:

$$B_{max} = 1.3\left[g_{HG}(\mu_{max})\Lambda_{aer}\right]^2 e^{-\tau\sqrt{m}}\left[e^{-\varphi/46} + 6me^{-\varphi/12}\right], \quad (8)$$

where $\mu_{max} = \cos\xi_{max}$.

Comparison of formula (8) with simulation results has shown that the error of the suggested approximation is 20%.

3. Method of AOD determination

It was already noted above that the sky brightness, depending on the viewing zenith angle, in the near-horizon zone has its maximum, which is almost fully determined by the total optical depth. This allowed us to suggest a new method of the atmospheric AOD determination from the zenith angle (different from 90°), at which the brightness maximum is observed.

To estimate the method applicability, we calculated interrelations between the atmospheric AOD and ξ_{max} for different viewing azimuth angles and model values of input parameters (Fig. 5).

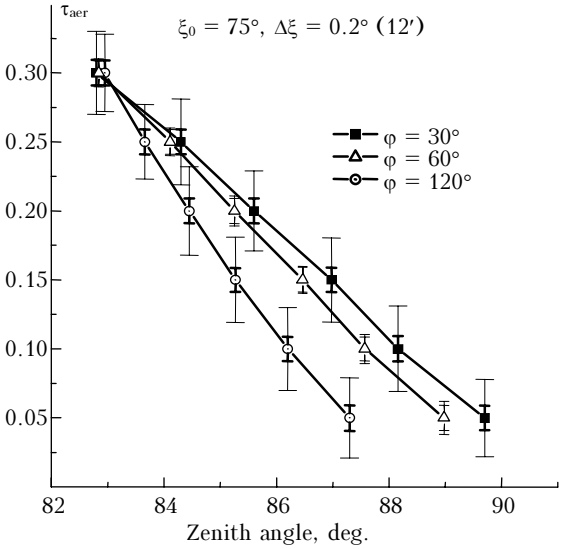

Fig. 5. Interrelation between atmospheric AOD and the zenith angle, at which the sky brightness maximum (ξ_{max}) is observed.

Vertical bars indicate errors in the AOD determination: a) inner bars reflect errors only due to inaccuracy in determination of the maximum angular position $\Delta\xi_{max} = \pm 0.2°$; and b) outer bars reflect the presence of additional error due to variations of optical characteristics derived from the model (scattering phase functions, single scattering albedo, and surface albedo A_S). The calculations show that the minimum error in the AOD determination (up to ±0.015) is realized in the region of scattering angles ~ 60°, where the aerosol scattering phase functions cross. This property of aerosol scattering phase functions is well known and is frequently used in angular methods of light scattering to minimize the influence of scattering phase function variations (see, e.g., Refs. 17 and 22). Therefore, to minimize the error in the AOD determination, it is necessary to use the initial formula (7a) for the forward hemisphere:

$$\tau_{aer} = \frac{89.5 + 7e^{-\varphi/60} - \xi_{max}}{29.7 + 0.8m - 0.11\varphi} - \tau_R. \qquad (9)$$

Based on results of field measurements of sky brightness zenith distributions, the developed method was tested and compared with the standard method[16] of AOD measurements from the direct solar radiation (Fig. 6).

The comparison results have shown a good agreement: the standard deviation of data obtained by the two methods is 0.013, and the cross-correlation coefficient is 0.83.

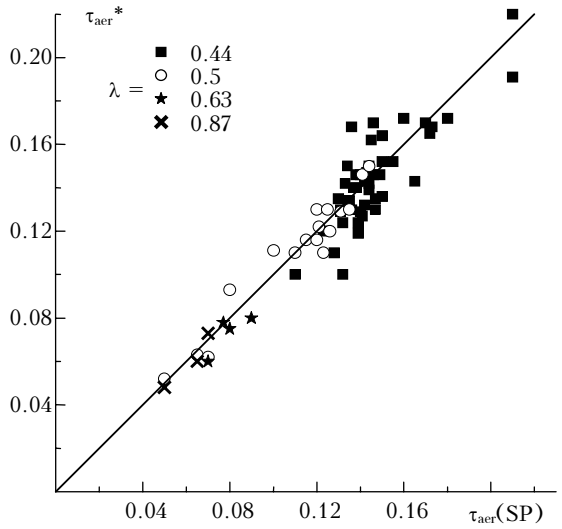

Fig. 6. Comparison of results of AOD determination by standard (τ_{aer}(SP)) and angular (τ_{aer}*) methods.

The advantage of the angular method considered here is that it does not require the absolute calibration. It is sufficient to make relative measurements of the sky brightness zenith distribution. The main difficulty in the use of the classical method ("transmission method") is in necessity of a qualitative calibration of the photometer, which should be made either at mountain observatories or on the base of accumulation of long-term observation series and subsequent careful selection of calibration situations. The developed method is not an alternative to the standard method; however, it can be used for control and rapid "calibration" of results obtained by the "transmission method."

One of limitations of the developed method is impossibility of its use under conditions of high atmospheric transmission ($\tau < 0.05$), when the angular position of the sky brightness maximum contracts to the horizon.

Conclusion

The results of experimental studies have confirmed that the numerical simulation algorithm developed earlier adequately describes the observed fields of the clear sky diffuse radiation at large viewing zenith angles.

The few-parameter models are constructed characterizing the sky brightness angular distribution near the horizon. Experimental tests have shown that for most observation situations the error of the proposed formulas does not exceed 15–20%. In the regions of large and small scattering angles ($\theta < 30°$ and $\theta > 150°$) this error can reach 25–35%.

We have proposed a new method of atmospheric AOD determination from the zenith angle magnitude, at which the sky brightness maximum above the horizon is observed. Experimental tests have shown that the angular method well agrees with independent measurements of the atmospheric AOD. The developed method can be used for fast calibration of photometers, which measure the AOD by the standard transmission method.

Acknowledgments

This work is supported by the Russian Foundation for Basic Research (grant No. 05–05–64410).

References

1. V.N. Glushko, A.I. Ivanov, G.Sh. Livshits, and I.A. Fedulin, *Scattering of Infrared Radiation in the Clear Atmosphere* (Nauka, Alma-Ata, 1974), 210 pp.
2. J. Lenoble, ed., *Radiative Transfer in Scattering and Absorbing Atmospheres: Standard Computational Procedures* (Deepak Publishing, Hampton, VA, 1985).
3. T.A. Sushkevich, S.A. Strelkov, and A.A. Ioltukhovskii, *Method of Characteristics in Problems of Atmospheric Optics* (Nauka, Moscow, 1990), 296 pp.
4. U.M. Sultangazin, *Spherical Harmonic Discrete Ordinate Methods in Problems of Kinetic Transport Theory* (Nauka, Alma-Ata, 1979), 268 pp.
5. T.A. Sushkevich, Atmos. Oceanic Opt. **12**, No. 3, 240–246 (1999).
6. M.A. Nazaraliev, *Statistical Simulation of Radiative Processes in the Atmosphere* (Nauka, Novosibirsk, 1990), 226 pp.
7. G.I. Marchuk, ed., *Monte Carlo Method in Atmospheric Optics* (Nauka, Novosibirsk, 1976), 283 pp.
8. O.T. Dubovik and M. King, J. Geophys. Res. D **105**, No. 16, 20673–20696 (2000).
9. T. Nakajima, G. Tonna, R. Rao, P. Boi, Y. Kaufman, and B. Holben, Appl. Opt. **35**, No. 15, 2672–2686 (1996).
10. M. Wang and R. Gordon, Appl. Opt. **32**, No. 24, 4598–4609 (1993).
11. T.B. Zhuravleva, I.M. Nasrtdinov, and S.M. Sakerin, Atmos. Oceanic Opt. **16**, Nos. 5–6, 496–504 (2003).
12. T.B. Zhuravleva, I.M. Nasrtdinov, S.M. Sakerin, K.M. Firsov, and T.Yu. Chesnokova, Atmos. Oceanic Opt. **16**, No. 12, 972–981 (2003).
13. S.M. Sakerin, T.B. Zhuravleva, and I.M. Nasrtdinov, Atmos. Oceanic Opt. **18**, No. 3, 222–231 (2005).
14. V.V. Sobolev, *Scattering of Light in Atmospheres of Planets* (Nauka, Moscow, 1972), 335 pp.
15. V.A. Smerkalov, *Applied Optics of the Atmosphere* (Gidrometeoizdat, St. Petersburg, 1997), 334 pp.
16. G.P. Gushchin, *Methods, Instruments, and Results of Measurements of Spectral Transmission of the Atmosphere* (Gidrometeoizdat, Leningrad, 1988), 200 pp.
17. E.V. Pyaskovskaya-Fesenkova, *Study of Light Scattering in the Earth's Atmosphere* (Izd. Akad. Nauk SSSR, Moscow, 1957), 219 pp.
18. *A Preliminary Cloudless Standard Atmosphere for Radiation Computation: World Climate Research Programme.* WCP-112, WMO/TD, No. 24 (1986), 60 pp.
19. G. Anderson, S. Clough, F. Kneizys, J. Chetwynd, and E. Shettle, *AFGL Atmospheric Constituent Profiles* (0–120 km), Air Force Geophysics Laboratory. AFGL-TR-86-0110, Environ. Res. Paper, No. 954 (1986).
20. http://aeronet.gsfc.nasa.gov
21. S.M. Sakerin and D.M. Kabanov, in: *Proc. 16th ARM Science Team Meeting* (Albuquerque, NM.) 2006, http://www.arm.gov/publications/proceedings/conf16/extended_abs/sakerin_sm.pdf
22. V.E. Pavlov and A.S. Shestukhin, Atmos. Oceanic Opt. **15**, Nos. 5–6, 381–382 (2002).